DEPARTMENT OF DEFENCE
DEFENCE SCIENCE & TECHNOLOGY ORGANISATION
DSTO

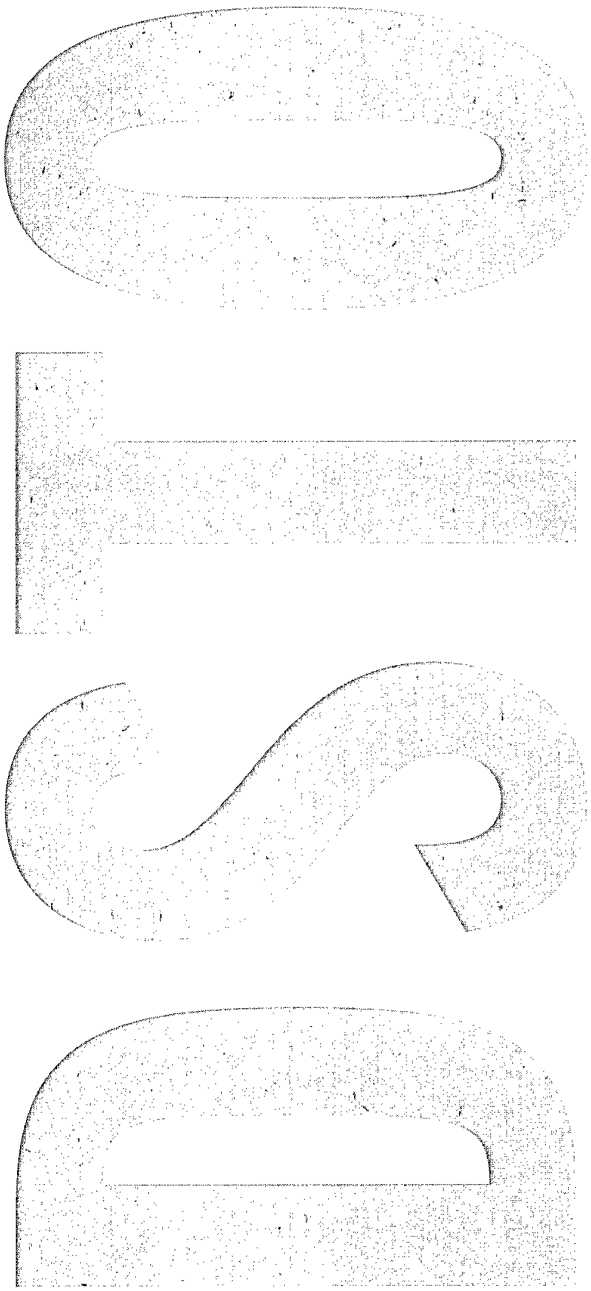

Stress Analysis of the F-111 Wing Pivot Fitting

S. Weller and M. McDonald

DSTO-TN-0271

Stress Analysis of the F-111 Wing Pivot Fitting

S. Weller and M. McDonald

Airframes and Engines Division
Aeronautical and Maritime Research Laboratory

DSTO-TN-0271

ABSTRACT

A number of high stress and potential cracking sites in the F-111 wing pivot fitting (WPF) have been identified using a validated 3D finite element model. Selected locations have been analysed in detail, and ranked according to the magnitude of the peak stress. These locations have also been compared with known sites of in-service cracking. Overall, there is very good agreement between the locations identified from the finite element model and those experiencing in-service cracking. The results from this investigation may assist the RAAF in reviewing inspection requirements for the F-111 WPF.

RELEASE LIMITATION

Approved for public release

DEPARTMENT OF DEFENCE
DEFENCE SCIENCE & TECHNOLOGY ORGANISATION
DSTO

Published by

DSTO Aeronautical and Maritime Research Laboratory
PO Box 4331
Melbourne Victoria 3001 Australia

Telephone: (03) 9626 7000
Fax: (03) 9626 7999

AR-011-422
April 2000

APPROVED FOR PUBLIC RELEASE

Stress Analysis of the F-111 Wing Pivot Fitting

Executive Summary

The wing pivot fitting (WPF) of the F-111 aircraft has experienced in-service fatigue cracking at a number of locations. Currently, the Royal Australian Air Force (RAAF) monitor a number of potential cracking sites in the WPF. It is possible that some sites are being monitored too rigorously, causing considerable undue expense for the RAAF. It is also possible that there exist potential cracking sites that are not included for inspection at all.

Recently, AMRL have acquired and developed a validated finite element (FE) model of the F-111 WPF. In this investigation the model has been used to identify potential cracking sites and list them in an approximate order of severity. The identified sites have been compared to in-service cracking experience and known durability and damage tolerance assessment (DADTA) control points.

In-service cracking has occurred in regions of reducing stiffener height known as stiffener runouts (SRO), and around elongated holes known as fuel flow vent holes (FFVH). These features can cause significant local stress concentrations and have been a main focus of this investigation.

The results confirm FFVH 13 and SRO 2U, which are current DADTA control points, as being the most severe locations in the WPF in terms of cracking potential. Other locations identified in the investigation which also have in-service cracking experience, are FFVHs 11, 12, and 14, and SROs 3U and 4U. Some of the locations identified during the investigation have not been the site of in-service cracking. These are FFVHs 15, 16, 57, and 58, SROs 5U and 3L, and the aft outboard edge of the lower plate.

Overall, there is very good agreement between the locations identified in this investigation and locations with in-service cracking experience. The results from this work are considered to be useful for the RAAF for the through-life management of the F-111 WPF.

It should be noted that this investigation only assesses the relative severity of selected locations based on stress level. To gain a more complete picture, a DADTA would be needed to establish the severity in terms of crack growth and inspection interval.

Contents

1. Introduction

The F-111 aircraft have experienced in-service cracking at a number of locations in the wing pivot fitting (WPF). Currently, the Royal Australian Air Force (RAAF) monitor a number of potential cracking sites in the WPF. It is possible that some sites are being monitored too rigorously, causing considerable undue expense for the RAAF. It is also possible that there exist potential cracking sites that are not included for inspection at all.

Recently, AMRL have acquired and developed a validated finite element (FE) model of the F-111 WPF [1, 2]. In this investigation the model has been used to identify potential cracking sites and list them in an approximate order of severity. The identified sites have been compared to in-service cracking experience and known durability and damage tolerance assessment (DADTA) control points. The results from this investigation may assist the RAAF in reviewing inspection requirements for the F-111 WPF.

2. Background

2.1 Wing Pivot Fitting

The location of the WPF is shown in Figure 1. It is designed to transmit wing loads to the wing carry through box, and as such it has high structural importance. The use of D6ac steel in its construction offers high strength but fairly low fracture toughness, making it sensitive to fatigue cracking, especially in areas of high stress concentration. To ensure the safety of the aircraft, in-service wings undergo extensive periodic inspections, and a periodic proof load test known as the cold proof load test (CPLT)[1]. The purpose of the CPLT is to confirm that any undetected cracks are not critical, thus clearing the aircraft for a further period of safe flight.

Application of CPLT loads (approximately design limit loads for the wing) causes localised yielding in some areas of high stress concentration in the WPF, leaving residual stresses in the yielded regions upon unloading. In particular, for positive CPLT loads, certain areas in the upper plate experience compressive yield, with the resultant residual stresses being tensile. It has been found that these residual tensile stresses are the main factor driving in-service fatigue cracks. Although the effect of residual stresses on crack growth rate is significant, it has only been considered qualitatively in this report.

---

[1] In CPLT the aircraft is cooled to -40°F to embrittle the D6ac steel structure, then loaded to -2.4 *g* and +7.33 *g* at 56° wing sweep angle followed by -3.0 *g* and +7.33 *g* at 26° wing sweep angle.

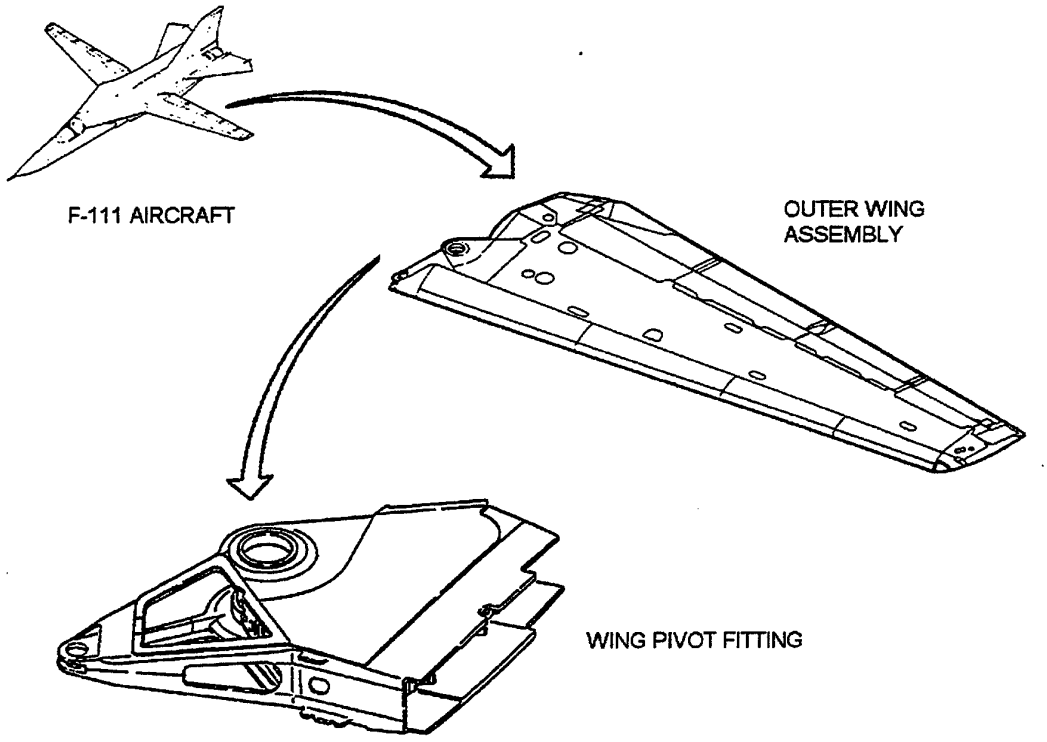

Figure 1: Location of the F-111 wing pivot fitting

Cracking has occurred in regions of reducing stiffener height known as stiffener runouts (SRO), and around elongated holes known as fuel flow vent holes (FFVH). Areas of local stress concentration, referred to here as 'hot spots', are predominantly found at FFVHs and SROs, hence these features have been a main focus of this investigation. Figure 2 shows the locations of all FFVHs and SROs in the WPF.

Two well-known critical sites in the upper plate of the WPF are FFVH 13 and SRO 2U[2]. Both exhibit very high stress concentrations and both have experienced numerous in-service cracks [3, 4, and 5]. Furthermore, these items are two of the control points for the F-111 DADTA. A significant amount of work has been directed toward managing these sites [4-11]. Recent instances of cracking at FFVHs 11 and 12 [12] indicate that other areas may also be cause for concern, especially as the aircraft moves into the latter stages of its planned operational life.

[2] The labelling of FFVHs and SROs used in this report follows that used in the aircraft structural repair manual, where 'U' and 'L' are used to differentiate between upper and lower plate stiffener runouts. SRO 2U is often referred to as simply SRO 2, or SRO#2.

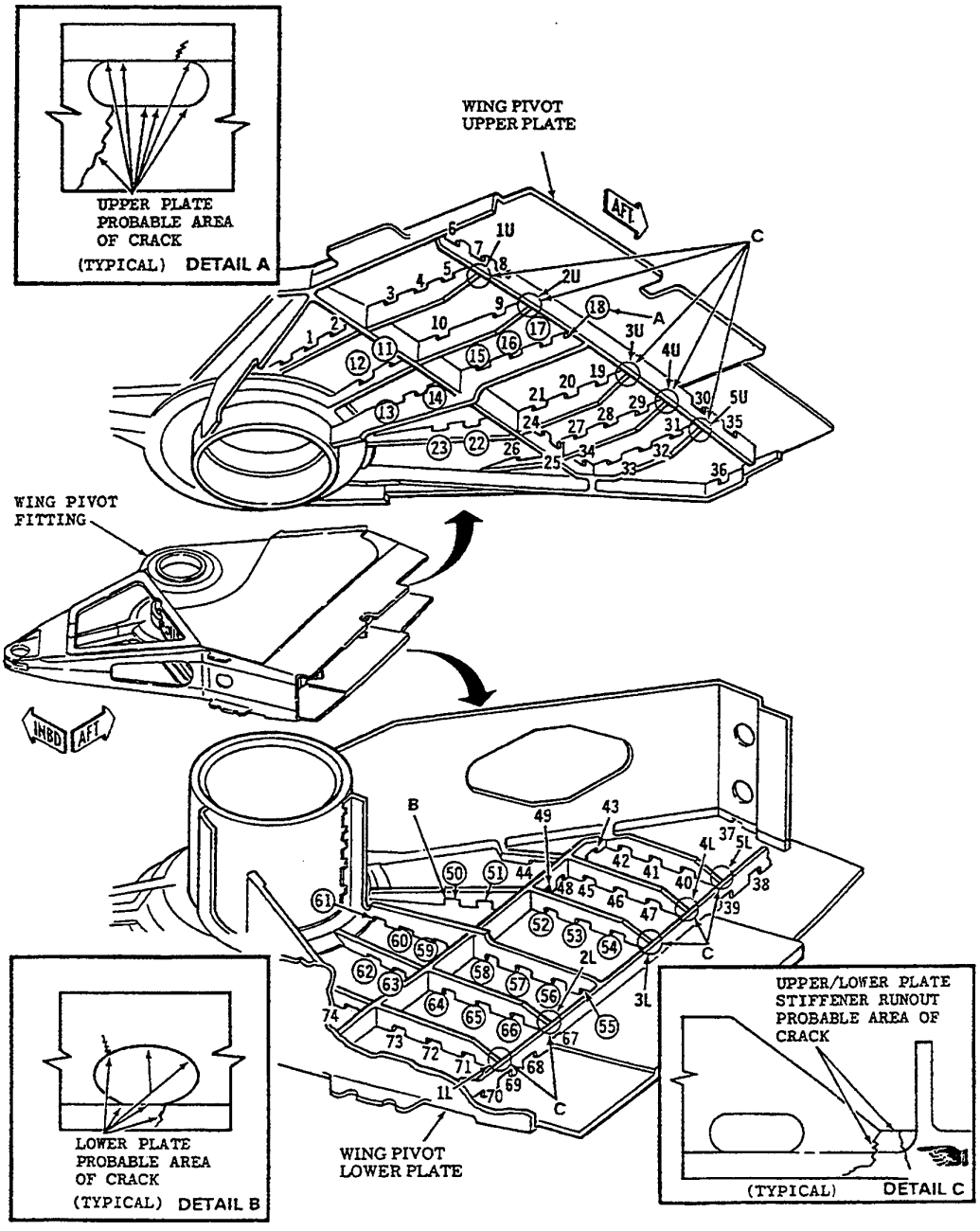

Figure 2: F-111 wing pivot fitting details

2.2 Finite Element Model

The original F-111 WPF FE model was supplied by Lockheed Martin Tactical Aircraft Systems (LMTAS) [1]. A section of the model is shown in Figure 3. It was designed to capture the internal load distribution within the WPF structure. The WPF structure is modelled in detail with virtually all WPF components represented using 3D solid elements. A small stub of wing is also coarsely modelled to help apply the wing loads to the WPF correctly. The model is configured with a lower plate boron doubler.

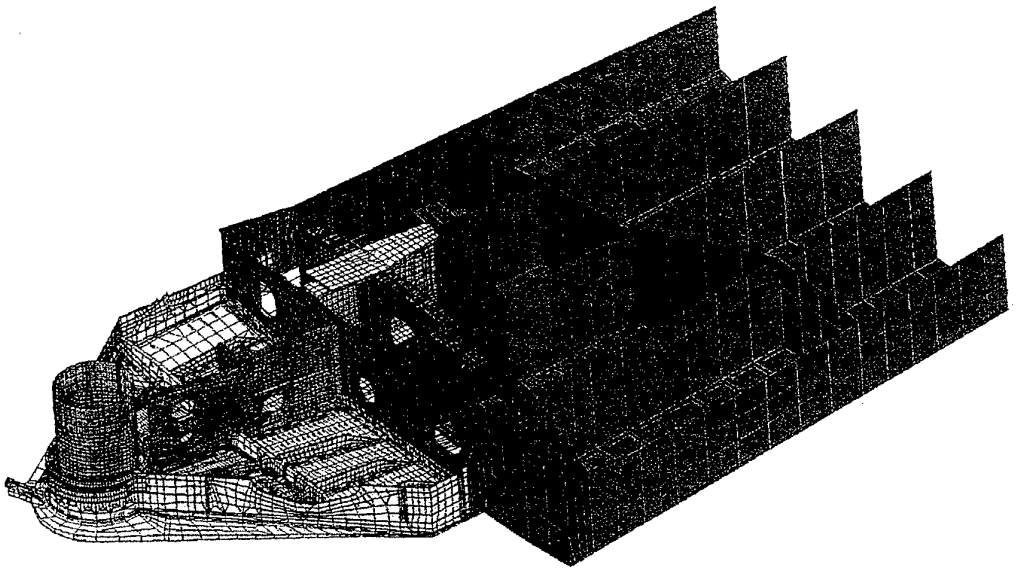

Figure 3: F-111 WPF finite element model

The mesh refinement is suitable for capturing the stiffness of the structure. It may also be used to obtain stresses and strains at far field locations not subject to high stress gradients. Due to the general coarseness of the mesh, it cannot capture accurate stress or strain results at local notch details such those found in the FFVHs and SROs.

This model has been validated with experimental results from an ex-USAF test wing [13]. As supplied, the model correlated well at far field locations such as the upper and lower plate. However, the strains near to FFVH 13 and the SROs correlated poorly. Consequently, AMRL has since made various enhancements to the model, and improved the correlation at FFVH 13 and SRO 2U significantly [2]. The current improved model was used as the base model for the study reported here.

Far field upper and lower plate strains from the current WPF FE model agree in general to within 10% of test results. The correlation is best toward the middle of the WPF (0% - 10% difference), and tends to degenerate at the fore and aft extremities (up to 30% difference). The FE strains on the integral WPF stiffeners also agree well with test results, the average difference being less than 10%. This includes stiffener #3, which contains FFVH 13. The FE strains near SRO 2U are also within 10% of test results. A similar correlation is expected at other SROs, however it is difficult to verify conclusively using the limited test results that are available.

The model is expected to be very useful for identifying hot spots in the structure. However, given that the level of correlation does vary somewhat across the model, direct comparison of stresses at each location should be interpreted with some discretion.

The FFVH and SRO profiles used for the investigation are shown in Appendix A. These are the profiles given by the assembly drawings for the WPF upper and lower plates, and they are labelled 'blueprint' to distinguish them from the range of profiles that have been implemented in the model for separate investigations.

3. Analysis Approach

The investigation was conducted in two parts. Firstly, the current FE model was used as is to identify potential cracking sites. All stress results for this part are termed 'preliminary'. Secondly, mesh improvements were made at selected hot spots to determine the peak stress so that they could be ranked in order of severity. All stress results for the second part are termed 'final'.

The load case used to compare peak stresses was the +7.33 g CPLT wing tip up condition. In general, this is the most severe loading for the WPF, and at isolated locations localised yielding can occur. The FE analyses reported here are linear elastic only - yielding is not modelled. However, the linear elastic results are still adequate for comparing the relative stress severity of hot spots.

4. Identification of Potential Cracking Sites

Prior to any mesh refinements, stress results were extracted from the current model to identify areas requiring further investigation. The peak von Mises stresses from each FFVH and SRO were tabulated. This, in combination with a qualitative visual

inspection of stress contour plots (Figures 4 and 5) and an examination of full-scale test data, was used to select the most severe locations.

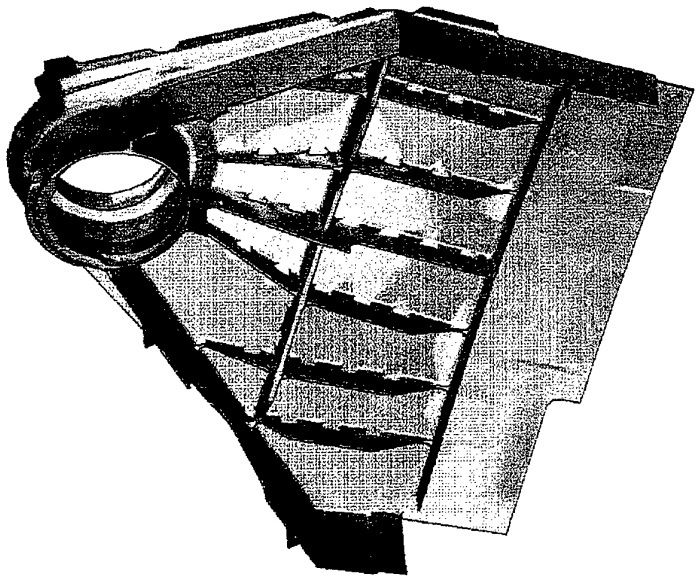

Figure 4: Stress contour plot of the WPF upper plate

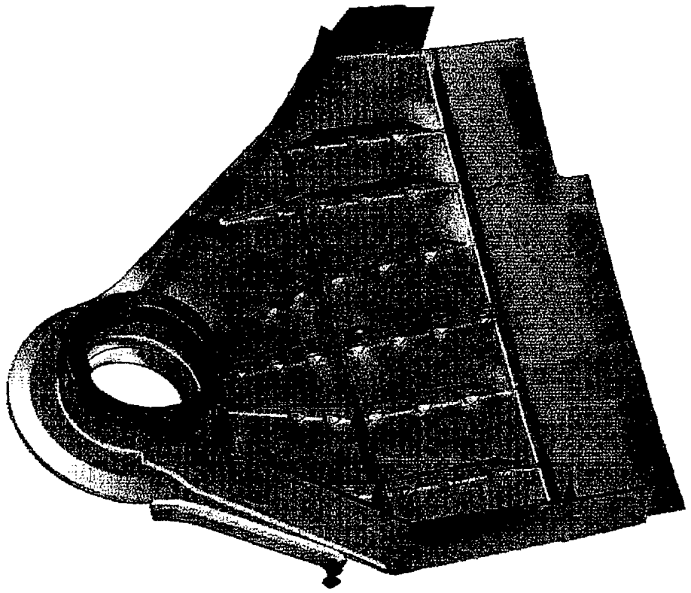

Figure 5: Stress contour plot of the WPF lower plate

The peak stresses occurred at locations along the FFVHs and SROs where in-service cracking also occurrs, as shown in Figure 2. These locations are the lower inboard corner of the upper plate FFVHs, the upper inboard corner of the lower plate FFVHs, and the corner radius of the SROs, both in the upper and lower plates. The upper plate peak stresses are compressive while the lower plate peak stresses are tensile.

It was noted that the quality and density of the FE mesh was not consistent across the selected locations, and as expected, the majority exhibited coarse meshes incapable of capturing the detail stress field. Nonetheless, qualitative inspection of the stress results was adequate to identify the hot spots.

Initially, all locations exhibiting stress levels above 80% of the relevant DADTA control point level[3] were included in the selected set. Since very few FFVHs met this criterion based on the preliminary results, the investigation was broadened to encompass a group of the next most severe vent holes.

Figures 6 and 7 show the preliminary peak stresses at each FFVH and SRO. The results are also tabulated in Appendix B. On the basis of these results the following items were selected for further investigation:

- FFVHs 11, 12, 13, 14, 15, and 16 in the WPF upper plate
- FFVHs 57 and 58 in the WPF lower plate
- SROs 2, 3, 4 in the WPF upper plate
- SRO 3 in the WPF lower plate

The location of these items in the WPF can be seen in Figure 2.

SRO 5 in the upper plate was also included in this group after a review of full-scale strain survey data [13]. For the +7.33 *g* load case the test data clearly shows yield conditions for this SRO similar to SRO 3 and SRO 4. This was not evident from the preliminary FE results.

The magnitude of the peak stress at SRO 3L is approximately 80% of the SRO 2U value and the stresses there are tensile for positive loads. Although it may experience a relatively high tensile spectrum during flight conditions, it is not considered as critical due to an expected residual compressive field after CPLT loading. This would have a beneficial effect on fatigue crack growth. A similar scenario would apply to all lower plate SROs. For this reason, no detail stress analysis has been performed at SRO 3L in this investigation, as it may be inappropriate to use the stress results alone to compare this location with upper plate SROs. A DADTA analysis, which would account for the residual compressive stress field, would be required in order to assess correctly its relative cracking potential.

[3] FFVH 13 for upper vent holes, FFVH 58 for lower vent holes, SRO 2U for runouts.

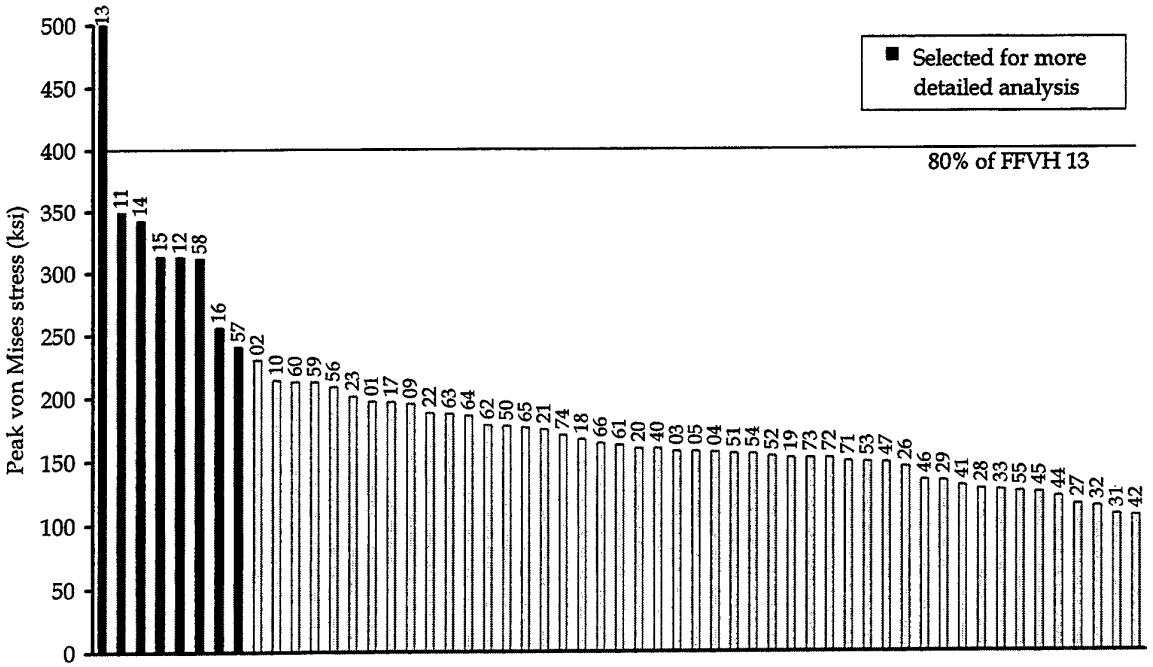

Figure 6: Preliminary peak stress results for each fuel flow vent hole (+7.33 g load case)

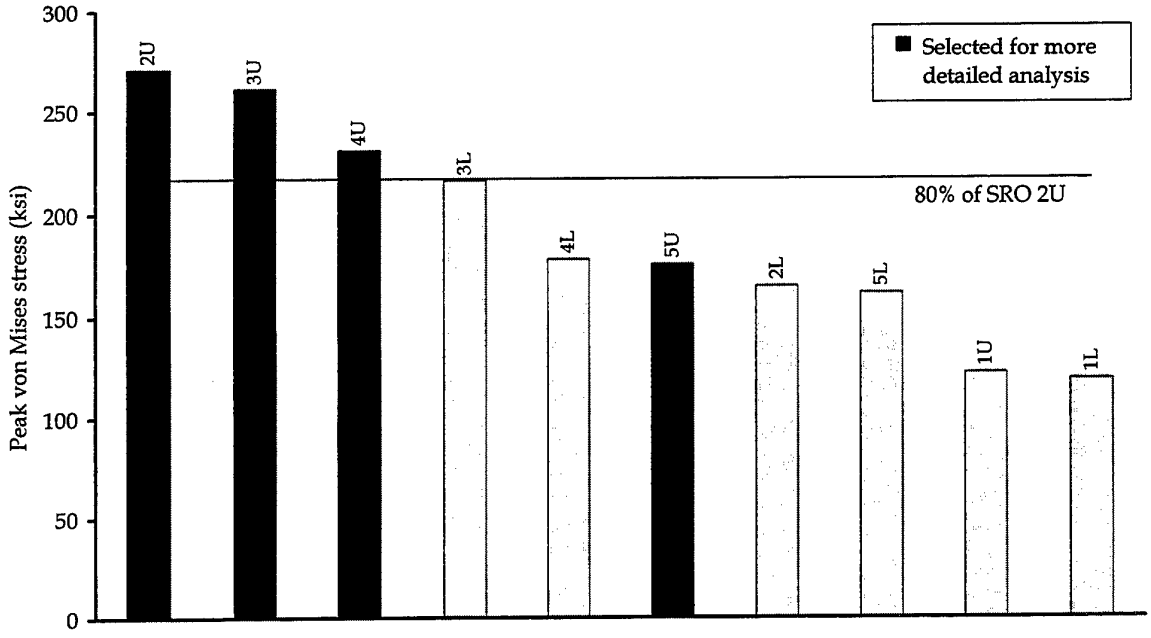

Figure 7: Preliminary peak stress results for each stiffener runout (+7.33 g load case)

One other area of relatively high stress indicated by the preliminary results is the aft edge of the lower plate immediately inboard of bulkhead 1.0 (Figure 8). The thickness of the lower plate increases from 0.185" inboard of the bulkhead to 0.295" where the plate joins the lower wing skin. The peak stress occurs in the fillet radius of this thickness change and is tensile. The von Mises stress of 238.8 ksi is comparable with the preliminary results for SRO 4U.

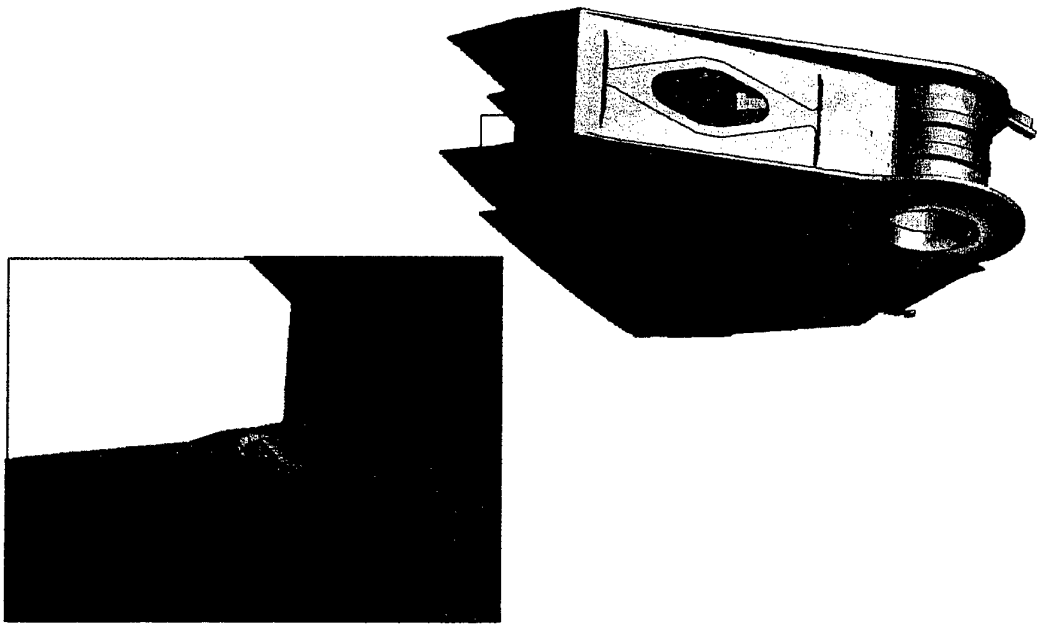

Figure 8: Localised stress peak in the aft edge of the lower plate

The cause of this stress peak has not been fully determined. An inspection of the FE model in this region reveals a complex meeting of parts, involving the WPF lower plate, the lower wing skin, bulkhead 1.0 and spars. This suggests that the stress peak could be a product of the way these parts and their connections have been approximated in the model. Alternatively it may be a real effect. It was noted that a comparison of far field lower plate strains in the vicinity indicates that the FE results overestimate full-scale test results by around 30%. Subsequently, this location was not investigated any further.

5. Detail Stress Analysis of Potential Cracking Sites

As mentioned previously, extensive mesh refinement was required at most of the selected hot spots to capture accurate peak stresses. In general, this involved replacing irregular or distorted elements and increasing the mesh density. Higher order elements, and convergence checks, were also applied to the areas of interest to ensure that mesh discretisation errors were minimised.

Figures 9 and 10 show typical stress contour plots for FFVH 13 and SRO 2U respectively.

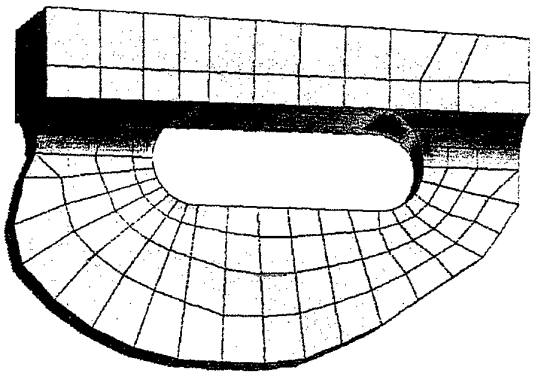

Figure 9: Stress contour plot of FFVH 13

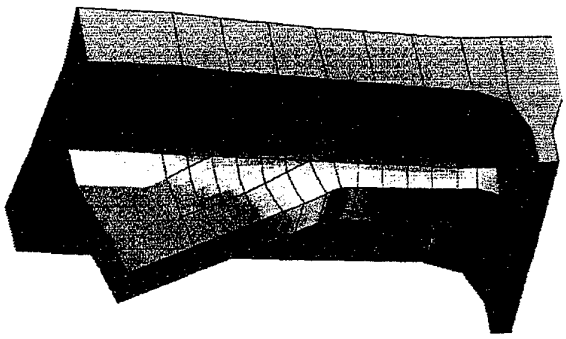

Figure 10: Stress contour plot of SRO 2U

5.1 Comparison of Selected Fuel Flow Vent Holes

Table 1 summarises the final peak von Mises stress at each FFVH as determined from the detail stress analysis. These are represented graphically in Figure 11, with the preliminary results included for comparison. As can be seen, the mesh improvements have resulted in a marked increase in the peak stress. For FFVHs 13 and 58 the increase is relatively small since the initial meshes at these locations were of reasonable quality. Conversely, there is a large increase in the peak stresses indicated at FFVHs 15 and 16, for which the initial meshes were very poor.

Table 1: Final peak stresses at selected fuel flow vent holes

FFVH	Peak von Mises Stress (ksi)	% of FFVH 13	In-service Cracking	DADTA Item
13	553.2	100	✓	✓
11	445.6	81	✓	
15	442.2	80		
14	427.4	77	✓	
12	410.4	74	✓	
16	371.3	67		
58	339.2	61		✓
57	318.7	58		

As expected FFVH 13 shows the most severe peak stress. FFVHs 11, 12, 14, and 15 exhibit approximately similar stress levels at about 80% of the FFVH 13 level. FFVH 16 is less severe at 67% while FFVHs 57 and 58 are around 60%.

For each upper plate FFVH (11 to 16) the peak stress occurs in the lower inboard corner, and is compressive for the load case considered. A significant but lesser peak (typically 80% of lower inboard value) is also evident in the upper outboard corner. For each lower plate FFVHs (57 and 58) the peak stress occurs in the upper inboard corner, and is tensile for the load case considered.

Table 1 also highlights vent holes that are known to have experienced in-service cracking in the RAAF fleet. Numerous cracks have been found at FFVH 13, while only a few cracks have been found at the other vent holes [3].

Direct comparison of peak elastic stress results between the upper and lower plate FFVHs may be inappropriate. This is because upper plate FFVH peaks are usually compressive, while lower plate FFVH peaks are usually tensile. This not only affects the sign of the normal operating stress, but also the residual stress induced after CPLT loading, which is known to have a considerable effect on crack growth rates. To fully

substantiate the relative cracking potential of all locations in the WPF a DADTA analysis would be required.

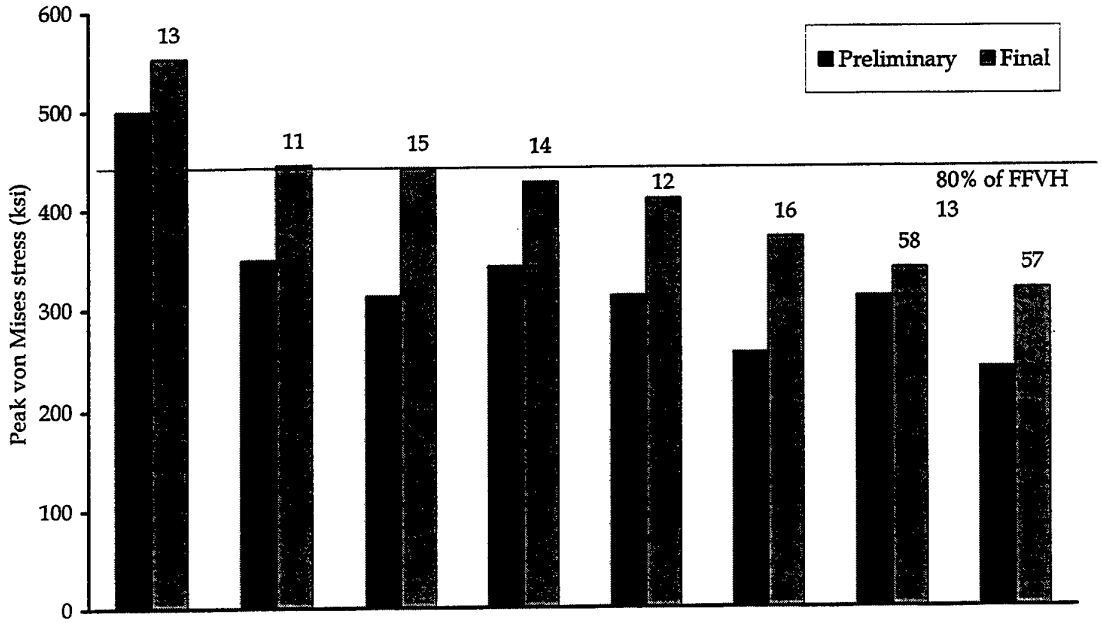

Figure 11: Preliminary and final peak stresses at selected FFVHs (+7.33 g load case)

5.2 Comparison of Selected Stiffener Runouts

Table 2 summarises the final peak von Mises stress at each SRO as determined from the detail stress analysis. The results are shown graphically in Figure 12, with the preliminary results included for comparison. As can be seen, SRO 2U is the most severe, followed by SRO 3U, SRO 4U and SRO 5U. The peak stresses at these SROs are compressive for the load case considered.

Table 2: Final peak stresses at selected stiffener runouts

SRO	Peak von Mises Stress (ksi)	% of SRO 2U	In-service Cracking	DADTA Item
2U	484.5	100%	✓	✓
3U	417.7	86%	✓	
4U	356.7	74%	✓	
5U	342.2	71%		

The detail peak stress results are much larger than the corresponding preliminary results with increases of up to 95%. This is due to the combined effect of the modelling adjustments in the SRO region and the very poor quality of the initial mesh.

Table 2 also highlights the runouts that are known to have experienced in-service cracking. Numerous cracks have been found at SRO 2U, while only a few cracks have occurred at the other runouts [3].

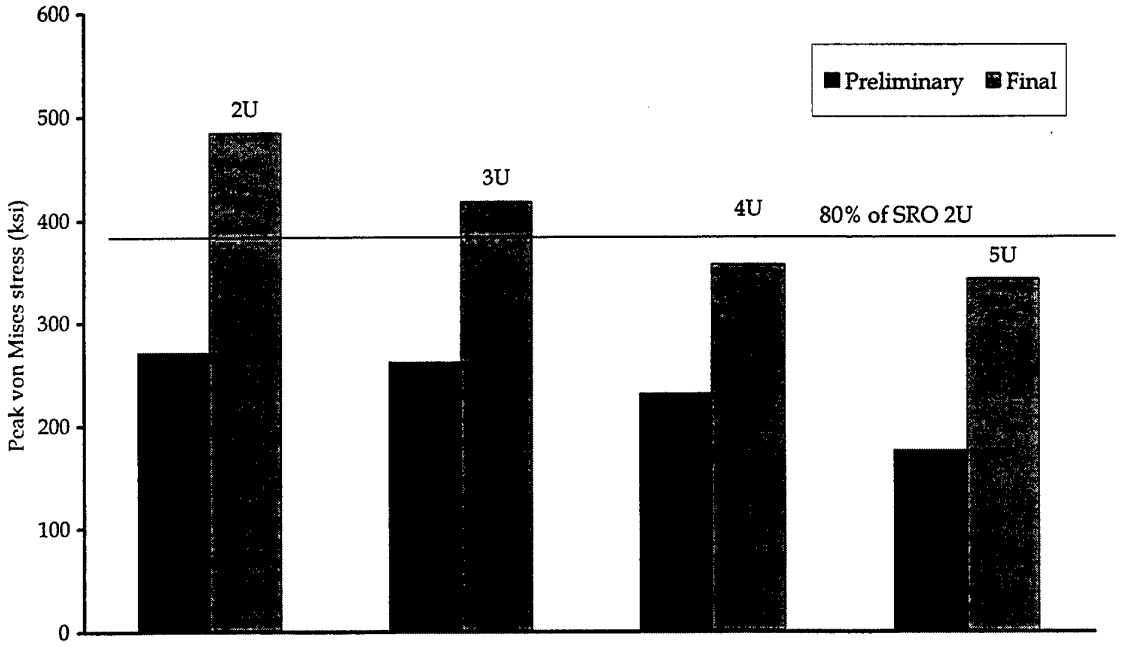

Figure 12: Preliminary and final peak stresses at selected SROs (+7.33 g load case)

6. Conclusion

This investigation presents a relative comparison of peak elastic stresses at potential cracking sites in the F-111 wing pivot fitting. The stress results were derived from the current validated FE model of the WPF.

The results confirm FFVH 13 and SRO 2U, which are current DADTA control points, as being the most severe locations in the WPF in terms of cracking potential. Other locations identified in the investigation which also have in-service cracking experience, are FFVHs 11, 12, and 14, and SROs 3U and 4U.

Some of the locations identified during the investigation have not been the site of in-service cracking. These are FFVHs 15, 16, 57, and 58, SROs 5U and 3L, and the aft outboard edge of the lower plate.

Overall, there is very good agreement between the locations identified in this investigation and locations with in-service cracking experience. The results from this work are considered to be useful for the RAAF for the through-life management of the F-111 WPF.

It should be noted that this investigation only assesses the relative severity of selected locations based on stress level. To gain a more complete picture a DADTA would be needed to establish the severity in terms of crack growth rate and inspection interval.

References

1. **Fuller, K. M.**, *The Wing Pivot Fitting Finite Element Model Final Report,* Lockheed Martin Tactical Aircraft Systems, USA, March 1997.

2. **McDonald, M., Maan, N. and Moras, F.**, *Validation and Enhancement of the F-111 Wing Pivot Fitting NASTRAN Finite Element Model,* DSTO Technical Report, File M1/9/772, Aeronautical and Maritime Research Laboratory, Melbourne, Australia, February 2000.

3. **Wilkin, M. O.**, *F-111 Aircraft Structural Integrity Management Plan,* Issue 1, Logistics Systems Agency, RAAF, Melbourne, Australia, April 1996.

4. **Cox, A. F.**, *Fatigue Cracking in the Upper Plate of Wing Pivot Fittings in F-111 Aircraft,* ARL-MAT-R-121, DSTO, Aeronautical and Maritime Research Laboratory, Melbourne, Australia, February 1988.

5. **Molent, L. and Swanton, G.**, *A Parametric Survey of Cracking in RAAF F-111C WPF Stiffeners,* ARL-TR-55, DSTO, Aeronautical and Maritime Research Laboratory, Melbourne, Australia, February 1994.

6. **Paul, J.**, *F-111 Stiffener Run Out #2 Parametric Study,* DSTO-TN-0104, Aeronautical and Maritime Research Laboratory, Melbourne, Australia, 1997.

7. **Watters, K. C.**, *Strain Surveys of Fuel Flow Vent Hole Number 13 and Stiffener Runout Number 2 in the F-111 Wing Pivot Fitting for a Range of Rework Shapes,* DSTO-TR-0567, Aeronautical and Maritime Research Laboratory, Melbourne, Australia, August 1997.

8. **Heller, M., McDonald M., Burchill, M., and Watters, K. C.** *Shape Optimisation of Critical Stiffener Runouts in the F-111 Wing Pivot Fitting,* DSTO Technical Report, File M1/9/680, Aeronautical and Maritime Research Laboratory, Melbourne, Australia, December 1999.

9. **Heller, M., Burchill, M, McDonald M. and Watters, K. C.** *Shape Optimisation of Critical Fuel Flow Vent Holes in the F-111 Wing Pivot Fitting,* DSTO Technical Report, File M1/9/679, Aeronautical and Maritime Research Laboratory, Melbourne, Australia, December 1999.

10. **Molent, L., Callinan, R. and Jones, R.**, *Structural Aspects of the Design of an All Boron/Epoxy Reinforcement for the F-111C Wing Pivot Fitting – Final Report,* ARL-RR-1, DSTO, Aeronautical and Maritime Research Laboratory, Melbourne, Australia, 1992.

11. **Lombardo, D., Graham, A. D. and Harris, F. G.,** *Stress Reduction in F-111 Wing Fuel Vent Holes by Using Neat-Fit Plugs - A Thermoelastic Analysis,* ARL-STRUC-TM-509, DSTO, Aeronautical and Maritime Research Laboratory, Melbourne, Australia, 1989.

12. **McDonald, M., and Watters, K. C.,** *Summary of Interim F-111 Wing Pivot Fitting Finite Element Investigations,* DSTO Technical Report, File M1/9/771, Aeronautical and Maritime Research Laboratory, Melbourne, Australia, February 2000.

13. **Lillingston, K.,** *F-111 Wing Variable Sweep Strain Survey,* Aeronautical & Maritime Research Laboratory, Structures Laboratory Report No. 8/95, DSTO, Melbourne, Australia, October 1995.

Appendix A: Blueprint Profiles

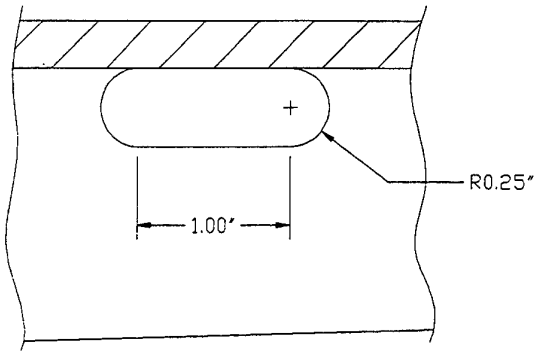

Figure 13: Blueprint profile for upper plate fuel flow vent holes

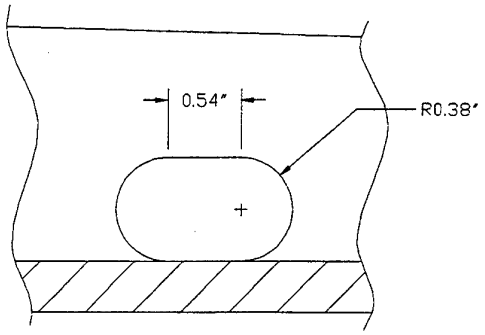

Figure 14: Blueprint profile for lower plate fuel flow vent holes

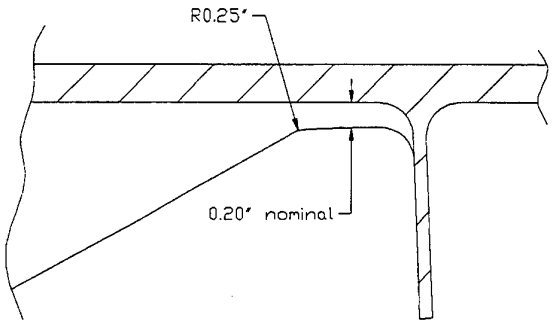

Figure 15: Blueprint profile for upper plate stiffener runouts

Appendix B: Preliminary peak stress results

This Appendix gives the preliminary peak von Mises stresses at each FFVH and SRO for the +7.33 *g* CPLT load case. Results were obtained from the Patran result file *wpf_003_2d_h0_results.db*.

Table A1: Preliminary peak stress results at each FFVH

FFVH	Peak σ_{VM} [ksi]	% of FFVH 13	Stress State	Node ID
13	500.2	100%	compressive	76979
11	349.0	70%	compressive	57171
14	342.3	68%	compressive	58040
15	313.0	63%	compressive	24066
12	312.6	62%	compressive	57287
58	311.4	62%	tensile	5808
16	255.9	51%	compressive	23834
57	240.7	48%	tensile	6584
02	230.1	46%	compressive	56847
10	213.8	43%	compressive	58591
60	212.5	42%	tensile	3908
59	212.4	42%	tensile	3780
56	208.4	42%	tensile	6647
23	201.0	40%	compressive	57572
01	196.9	39%	compressive	57008
17	196.3	39%	compressive	23718
09	194.8	39%	compressive	58655
22	187.7	38%	compressive	57428
63	186.8	37%	tensile	1243
64	185.4	37%	tensile	5250
62	177.7	36%	tensile	1219
50	176.9	35%	tensile	7491
65	175.7	35%	tensile	5284
21	174.4	35%	compressive	24470
74	169.8	34%	tensile	1256
18	166.5	33%	compressive	24009
66	163.4	33%	tensile	5382
61	161.9	32%	tensile	34222
20	159.2	32%	compressive	24339
40	159.1	32%	tensile	15428
03	157.1	31%	compressive	23339
05	157.1	31%	compressive	23455
04	156.3	31%	compressive	23571
51	155.2	31%	tensile	7392

Table A1: Preliminary peak stress results at each FFVH, continued

FFVH	Peak σ_{VM} [ksi]	% of FFVH 13	Stress State	Node ID
54	155.0	31%	tensile	11670
52	153.0	31%	tensile	11208
19	151.8	30%	compressive	24569
73	151.8	30%	tensile	8312
72	151.6	30%	tensile	8555
71	149.1	30%	tensile	8798
53	148.4	30%	tensile	11431
47	148.2	30%	tensile	12691
26	144.6	29%	compressive	57768
46	134.2	27%	tensile	12547
29	133.9	27%	compressive	25041
41	129.8	26%	tensile	15433
28	127.1	25%	compressive	24861
33	126.5	25%	compressive	25553
55	125.2	25%	tensile	6397
45	124.7	25%	tensile	12421
44	121.2	24%	tensile	2603
27	115.2	23%	compressive	24975
32	113.6	23%	compressive	25321
31	107.0	21%	compressive	25437
42	106.0	21%	tensile	15439

Table A2: Preliminary peak stress results at each SRO

SRO	Peak σ_{VM} [ksi]	% of SRO 2U	Stress State	Node ID
2U	270.8	100%	compressive	158028
3U	261.0	96%	compressive	25951
4U	230.5	85%	compressive	25889
3L	215.8	80%	tensile	12013
4L	178.1	66%	tensile	13355
5U	175.5	65%	compressive	25791
2L	164.7	61%	tensile	5356
5L	161.5	60%	tensile	14521
1U	122.2	45%	compressive	23689
1L	119.1	44%	tensile	8839

Stress Analysis of the F-111 Wing Pivot Fitting

S. Weller and M. McDonald

AUSTRALIA

DEFENCE ORGANISATION

Task Sponsor **DGTA**

S&T Program

Chief Defence Scientist
FAS Science Policy
AS Science Corporate Management
} shared copy
Director General Science Policy Development
Counsellor Defence Science, London (Doc Data Sheet)
Counsellor Defence Science, Washington (Doc Data Sheet)
Scientific Adviser to MRDC Thailand (Doc Data Sheet)
Scientific Adviser Policy and Command
Navy Scientific Adviser (Doc Data Sheet and distribution list only)
Scientific Adviser - Army (Doc Data Sheet and distribution list only)
Air Force Scientific Adviser
Director Trials

Aeronautical and Maritime Research Laboratory
Director

Chief of Airframes and Engines Division
Research Leader (Fracture Mechanics)
Kevin Watters
Tom van Blaricum
Kevin Walker
Manfred Heller
Marcus McDonald (5 copies)
Steve Weller

DSTO Library and Archives
Library Fishermans Bend
Library Maribyrnong
Library Salisbury (2 copies)
Australian Archives
Library, MOD, Pyrmont (Doc Data sheet only)
*US Defense Technical Information Center, 2 copies
*UK Defence Research Information Centre, 2 copies
*Canada Defence Scientific Information Service, 1 copy
*NZ Defence Information Centre, 1 copy
National Library of Australia, 1 copy

Capability Systems Staff
Director General Maritime Development (Doc Data Sheet only)
Director General C3I Development (Doc Data Sheet only)

Director General Aerospace Development

Army

ABCA Standardisation Officer, Puckapunyal, (4 copies)

SO (Science), DJFHQ(L), MILPO Enoggera, Queensland 4051 (Doc Data Sheet only)

Air Force

CENGR, 501 Wing, Amberley

ASI2 (FltLt P. Connor)

ASI2A (FltLt J. Davern)

OICASF, 501 Wing, Amberley (FltLt P. Birt)

Intelligence Program

DGSTA Defence Intelligence Organisation

Manager, Information Centre, Defence Intelligence Organisation

Corporate Support Program

OIC TRS, Defence Regional Library, Canberra

SPARES (5 copies)

Total number of copies: **47**

DEFENCE SCIENCE AND TECHNOLOGY ORGANISATION
DOCUMENT CONTROL DATA

1. PRIVACY MARKING/CAVEAT (OF DOCUMENT)

2. TITLE

Stress Analysis of the F-111 Wing Pivot Fitting

3. SECURITY CLASSIFICATION (FOR UNCLASSIFIED REPORTS THAT ARE LIMITED RELEASE USE (L) NEXT TO DOCUMENT CLASSIFICATION)

Document	(U)
Title	(U)
Abstract	(U)

4. AUTHOR(S)

S. Weller and M. McDonald

5. CORPORATE AUTHOR

Aeronautical and Maritime Research Laboratory
PO Box 4331
Melbourne Vic 3001 Australia

6a. DSTO NUMBER	6b. AR NUMBER	6c. TYPE OF REPORT	7. DOCUMENT DATE
DSTO-TN-0271	AR-011-422	Technical Note	April 2000

8. FILE NUMBER	9. TASK NUMBER	10. TASK SPONSOR	11. NO. OF PAGES	12. NO. OF REFERENCES
M1/9/711	96/102	DGTA	20	13

13. URL on World Wide Web
http://www.dsto.defence.gov.au/corporate/reports/DSTO-TN-0271.pdf

14. RELEASE AUTHORITY

Chief, Airframes and Engines Division

15. SECONDARY RELEASE STATEMENT OF THIS DOCUMENT

Approved for public release

OVERSEAS ENQUIRIES OUTSIDE STATED LIMITATIONS SHOULD BE REFERRED THROUGH DOCUMENT EXCHANGE, PO BOX 1500, SALISBURY, SA 5108

16. DELIBERATE ANNOUNCEMENT

No Limitations

17. CASUAL ANNOUNCEMENT Yes

18. DEFTEST DESCRIPTORS

F-111 aircraft, Wing pivot fittings, Fatigue life, Cracking (fracturing), Stress analysis, Finite element analysis, Holes (openings)

19. ABSTRACT

A number of high stress and potential cracking sites in the F-111 wing pivot fitting (WPF) have been identified using a validated 3D finite element model. Selected locations have been analysed in detail, and ranked according to the magnitude of the peak stress. These locations have also been compared with known sites of in-service cracking. Overall, there is very good agreement between the locations identified from the finite element model and those experiencing in-service cracking. The results from this investigation may assist the RAAF in reviewing inspection requirements for the F-111 WPF.